

# Solar cycle dependent characteristics of the equatorial blanketing $E_s$ layers and associated irregularities

C. V. Devasia, V. Sreeja, and S. Ravindran

Space Physics Laboratory, Vikram Sarabhai Space Centre, Trivandrum, 695022, India

Received: 5 April 2006 – Revised: 29 August 2006 – Accepted: 13 September 2006 – Published: 21 November 2006

**Abstract.** The occurrence of blanketing type  $E_s$  ( $E_{sb}$ ) layers and associated E-region irregularities over the magnetic equatorial location of Trivandrum ( $8.5^\circ$  N;  $77^\circ$  E; dip  $\sim 0.5^\circ$ ) during the summer solstitial months of May, June, July and August has been investigated in detail for the period 1986–2000 to bring out the variabilities in their characteristics with the solar cycle changes. The study has been made using the ionosonde and magnetometer data of Trivandrum from 1986–2000 along with the available data from the 54.95 MHz VHF backscatter radar at Trivandrum for the period 1995–2000. The appearance of blanketing  $E_s$  layers during these months is observed to be mostly in association with the occurrence of afternoon Counter Electrojet (CEJ) events. The physical process leading to the occurrence of a CEJ event is mainly controlled by the nature of the prevailing electro dynamical/neutral dynamical conditions before the event. Hence it is natural that the  $E_{sb}$  layer characteristics like the frequency of occurrence, onset time, intensity, nature of gradients in its top and bottom sides etc are also affected by the nature of the background electro dynamical /neutral dynamical processes which in turn are strongly controlled by the solar activity changes. The occurrence of  $E_{sb}$  layers during the solstitial months is found to show very strong solar activity dependence with the occurrence frequency being very large during the solar minimum years and very low during solar maximum years. The intensity of the VHF radar backscattered signals from the  $E_{sb}$  irregularities is observed to be controlled by the relative roles of the direction and magnitude of the prevailing vertical polarization electric field and the vertical electron density gradient of the prevailing  $E_{sb}$  layer depending on the phase of the solar cycle. The gradient of the  $E_{sb}$  layer shows a more dominant role in the generation of gradient instabilities during solar minimum periods while it is the electric field that has a more dominant role during solar maximum periods.

**Keywords.** Ionosphere (Electric fields and currents; Equatorial ionosphere; Ionospheric irregularities)

Correspondence to: C. V. Devasia  
(cv\_devasia@vssc.gov.in)

## 1 Introduction

Equatorial ionograms show the presence of layer type irregularities in the ionospheric E-region known as “Equatorial sporadic E” ( $E_{sq}$ ). They are dense layers or patches of ionization observed at heights of 100–120 km.  $E_s$  ( $E_{sq}$  over the equator) can occur during daytime or nighttime, and its characteristics vary markedly with latitude.  $E_s$  can be associated with thunderstorms, lightning, meteor showers, solar activity and geomagnetic activity and the main source of  $E_s$  for low-latitudes is wind shears. Near the magnetic equator, the  $E_s$  observed is patchy and transparent to waves reflected from the higher layers (Rishbeth and Garriott, 1969). Its presence is strongly associated with the day-time “Equatorial Electrojet” (EEJ), which consists of an enhanced flow of current over the magnetic equator in the eastward direction driven basically by a large vertical polarization electric field ( $E_p$ ) set up by the eastward electric field ( $E_y$ ) which has its origin in the global wind dynamo electric fields (Reddy, 1989; Stening, 1995). The equatorial  $E_s$  irregularities are highly field-aligned as shown experimentally by Kudeki et al. (1989), and are caused by plasma instabilities arising from the flow of large electrojet current (Rishbeth and Garriott, 1969). The  $E_s$  irregularities give rise to strong backscattered signals when probed by VHF/HF radars.

Basically there are two types of plasma instabilities that give rise to the electrojet irregularities. The first one, known as the two-stream instability, gives rise to type I radar spectra of the backscattered signals from the irregularities when the electrojet current is very strong so that the relative drift velocity between the electrons and the ions in the EEJ region exceeds the ion-acoustic velocity in the medium (Farley, 1963; Buneman, 1963). The second one, known as the “cross field” or gradient drift plasma instability gives rise to type II radar spectra when there exists a vertical electron density gradient, parallel to the direction of the vertical polarization electric field which drives the electrojet current flow (Balsley, 1973). The generation of the gradient drift plasma instability is responsible for the normal daytime layer type irregularities known as equatorial  $E_s$  ( $E_{sq}$ ) seen in the ionograms. This is consistent with the observation that the  $E_{sq}$

layers disappear at certain times of the day, when the normal eastward flow of the electrojet current gets reversed to a westward flow (Rastogi et al., 1971; Krishna Murthy and Sen Gupta, 1972; Mayaud, 1977; Rastogi, 1989; Reddy, 1989). This phenomenon as indicated by a depression in the horizontal component of the earth's magnetic field below its nighttime value is known as "Counter Electrojet" (CEJ) event.

Linear theories have been successful in determining the case of most E-region irregularities seen by coherent scatter radars at low and high latitudes; the most prominent among them being the Farley-Buneman mechanism (Farley, 1963; Buneman, 1963) and the gradient drift instability (Rogister and Angelo, 1970). Generation of large-scale irregularities in the unstable electrojet was first observed by radar observations at the Jicamarca Observatory in Peru (Farley and Balsley, 1973; Balsley and Farley, 1973; Farley et al., 1978; Farley, 1985). The 50 MHz radar echoes from 3 m irregularities can also act as tracers of the large-scale irregularities traveling in the zonal and vertical direction. More recently, these large-scale irregularities have been studied using radar interferometry techniques with one or more east-west base lines (Kudeki et al., 1982, 1985, 1987; Kudeki and Sürücü, 1991).

During CEJ events, the reversed flow of currents due to the downward polarization electric field  $E_p$  would not be able to destabilize the plasma to generate the type II irregularities in the presence of a vertically upward electron density gradient. Type II irregularities will be generated under normal EEJ/CEJ conditions only when both the vertical polarization electric field and the vertical electron density gradient are parallel and they can be observed by the VHF backscatter radars by the strong scattered echoes. During CEJ events, as the vertical polarization electric field is downward, type II spectra are observed only in the presence of a downward (negative) electron density gradient, a condition which is not achievable in normal E-layer during daytime.

During certain CEJ events, simultaneous appearance of very thin layers of enhanced ionization with both positive and negative gradients and effectively blanketing the F-layer of the ionosphere over Trivandrum has been observed (Reddy, 1989). These are known as Blanketing  $E_s$  ( $E_{sb}$ ) layers. The above facts imply that, just as the daytime electrojet is a seat of both type I and type II irregularities associated with the  $E_s$ , the CEJ on certain occasions can also be a seat of type I and type II irregularities associated with  $E_{sb}$  (Crochet et al., 1979; Somayajulu et al., 1994; Woodman and Chau, 2002; Devasia et al., 2004).

The blanketing frequency of the  $E_s$ -layer often denoted, as  $f_b E_s$  is the minimum frequency at which the F-region trace becomes visible in the ionograms. It is closely related to the maximum plasma frequency of the  $E_s$  layer.  $E_{sb}$  appear in the form of thin layers of enhanced ionization with sharp electron density gradients on either side that provide the basic requirement for the generation and growth of the gradient drift instabilities in the presence of crossed electric and mag-

netic fields. During the hours of upward polarization electric field (due to eastward electric field,  $E_y$ ) in daytime, the electron density gradient of the bottom side of the E region is adequate to sustain the gradient instabilities. But as the polarization electric field becomes weaker, the instabilities decay and finally disappear in the late afternoon hours. Under such conditions, if an  $E_{sb}$  layer is formed in the electrojet region, the sharp gradients associated with it leads to the buildup of the plasma irregularities to very large levels (sometimes even exceeding the peak noontime level usually observed in the presence of normal  $E_s$  layer) even when the electric field is weak. As the electric field approaches zero value the plasma instabilities decay and disappear, and they grow again as the field builds up strength after reversal if the  $E_{sb}$  layer persists (Reddy and Devasia, 1977).

The occurrence of  $E_{sb}$  layers in association with the appearance of CEJ events is quite frequent during the summer solstitial months of May, June, July and August over Trivandrum, India (Devasia, 1976). However, the observation of type II irregularities during CEJ events using the 54.95 MHz VHF radar at Trivandrum has been relatively infrequent and such observations are in general associated with the appearance of very sharp ionization layers or  $E_{sb}$  layers manifested by the Trivandrum ionograms (Reddy and Devasia, 1977; Somayajulu and Viswanathan, 1987; Reddy, 1989; Devasia et al., 2004).

Theoretical investigations in the past to explain physical processes that generate CEJ events have been based on two different approaches. In one approach (Richmond, 1973; Reddy and Devasia, 1981; Stening, 1985; Anandarao and Raghavarao, 1987), it was suggested that the local interaction of height varying zonal winds with the electrojet plasma could generate polarization electric fields of sufficient magnitude and direction which in turn can modify the latitudinal and height structure of the electrojet current. The generation of a CEJ event can thus be viewed as resulting from an extreme case of wind interaction with the electrojet causing large wind generated polarization electric field (negative) to reduce the normal polarization electric field (due to  $E_y$ ) in the EEJ. In a different approach, the possible reversal of the east-west electric field ( $E_y$ ) in the electrojet region due to an abnormal combination of tidal modes has been shown to produce a CEJ event (Forbes and Lindzen, 1976a, b; Marriott et al., 1979; Hanuise et al., 1983; Stening et al., 1996).

The physical mechanism responsible for the generation of  $E_{sb}$  layers over the magnetic equator was proposed to be due to the horizontal convergence of ionization due to horizontal shears in the horizontal neutral winds and it was also shown that the horizontal wind shears of required magnitude were being provided by the internal gravity waves of short period (Reddy and Devasia, 1973). However a later study by Reddy and Devasia (1981) showed that the local action of the east west winds with large vertical shears on the electrojet plasma could be responsible for the generation of the  $E_{sb}$  layers. These vertical shears result in the generation

of substantial wind induced polarization electric fields ( $E_w$ ) (Reddy and Devasia, 1981). The wind-induced polarization electric fields in the same direction as the vertical polarization electric field due to  $E_y$  can lead to the ionization convergence and hence the eventual formation of the  $E_{sb}$  layers. This establishes the close linkage between the generation of a CEJ event and the simultaneous appearance of an associated blanketing  $E_s$  layer as resulting from the local interaction of east-west winds with large vertical shears with the electrojet plasma when the electrojet is of comparatively lower intensity in the afternoon hours. Such favorable conditions appear to exist in the magnetic equatorial location of Trivandrum during the summer solstitial months of May, June, July and August.

In this paper we present a detailed study of some of the morphological and physical aspects of the occurrence of blanketing  $E_s$  layers over the magnetic equator at Trivandrum during the solstitial months of different years of 1986–2000. Here an attempt is made to bring out the solar cycle dependence of the various associated parameters and their control on the generation and general characteristics of the blanketing  $E_s$  and the associated E-region irregularities. The competing roles of the electric field and wind in the electrojet region on the occurrence characteristics of  $E_{sb}$  layers in response to the variabilities of the solar cycle are also discussed.

## 2 Data

For the present study, we have made use of the ionograms from the DIGITAL IONOSONDE MODEL IPS-42 at Trivandrum for the period of 1986–2000 to obtain the various characteristics of the blanketing  $E_s$  events over the magnetic equator during the solstitial months of each year. We have mainly used the regular 15 min interval ionograms during the above period for the study of the  $E_{sb}$  layer characteristics under the varying solar activity levels. The related characteristics of the daytime EEJ and CEJ have been studied using the hourly values of the horizontal component of the earth's magnetic field at Trivandrum (TIR) and Alibag (ABG; geographic latitude  $18.6^\circ$  N; geographic longitude  $72.9^\circ$  E; dip  $12.8^\circ$  N), a station outside the electrojet. All the  $E_{sb}$  cases during the solstitial months of May, June, July and August of each year were invariably found to be associated with the presence of a CEJ event. This was ascertained from the negative excursion in the variation of  $\Delta H_{TIR} - \Delta H_{ABG}$ , where  $\Delta H_{TIR}$  and  $\Delta H_{ABG}$  are respectively the daily variations in the geomagnetic field intensities ( $\Delta H$ ) above the nighttime levels at Trivandrum and Alibag. The parameter  $\Delta H_{TIR} - \Delta H_{ABG}$  at any time is an indicator of the EEJ strength. In addition to the ionograms and magnetograms, we have also used the available data during 1995–2000 from the 54.95 MHz VHF radar observations at Trivandrum to characterize some of the observed features of the type II irregu-

larities associated with the EEJ and CEJ in the context of the present study.

In the case of the type II irregularities observed by the radar the mean Doppler frequency ( $\bar{f}_D$ ) variation of the backscattered signals is proportional to the phase velocity of the 2.7 m scale size irregularities (corresponding to half the radar wavelength  $\lambda_r$  of 54.95 MHz) and this velocity in turn is proportional to the vertical polarization electric field due to the  $E_y$  field in the electrojet region (Fejer and Kelley, 1980). The parameter ( $\bar{f}_D$ ) is related to the east west drift velocity ( $V_p$ ) of the irregularities as:

$$V_p(\text{m/s}) = \frac{\lambda_r}{2} \cdot \bar{f}_D(\text{Hz}) \quad (1)$$

where  $\lambda_r = 5.4$  m, corresponding to the 54.95 MHz VHF radar at Trivandrum.

## 3 Observed features of $E_{sb}$ layers over the magnetic equator

The period 1986–2000 is characterized by two solar minimum and one maximum phases of the solar cycle. This has helped us to investigate the general features of the  $E_{sb}$  layer formation in response to the variation of the solar activity from minimum to maximum and back. The results are presented and discussed in terms of the observed average features of  $E_{sb}$  occurrences for each year of the period, thereby bringing out the pattern of solar cycle variation of the relevant parameters related to these events.

### 3.1 Comparison of noontime E-region electric field variations during equinoctial and solstitial periods of the solar cycle

The daytime east-west electric field ( $E_y$ ), in the equatorial electrojet, shows a strong seasonal dependence with its magnitude being much larger during the equinoctial period in comparison to that during the solstitial period. Also the equinoctial period (March–April months) in general has been found to be free from the occurrence of CEJ events and blanketing  $E_s$  events at Trivandrum. This seasonal preference for the occurrence of CEJ events and  $E_{sb}$  layers stems from the distinctly different characteristics of the ambient daytime electrodynamical conditions in the electrojet prevailing on each day of these seasons. The occurrence of CEJ events is the result of electrodynamical processes taking place under weakened EEJ conditions. The formation of  $E_{sb}$  layers in association with CEJ events give rise to gradient drift instability under the favorable conditions determined by the direction of the electron density gradients of the  $E_{sb}$  layer and the direction of the vertical polarization electric field prevailing at this time. Both the strength of the noontime east-west electric field ( $E_y$ ) in the EEJ region and the nature of its variation in the afternoon hours, while showing a strong seasonal

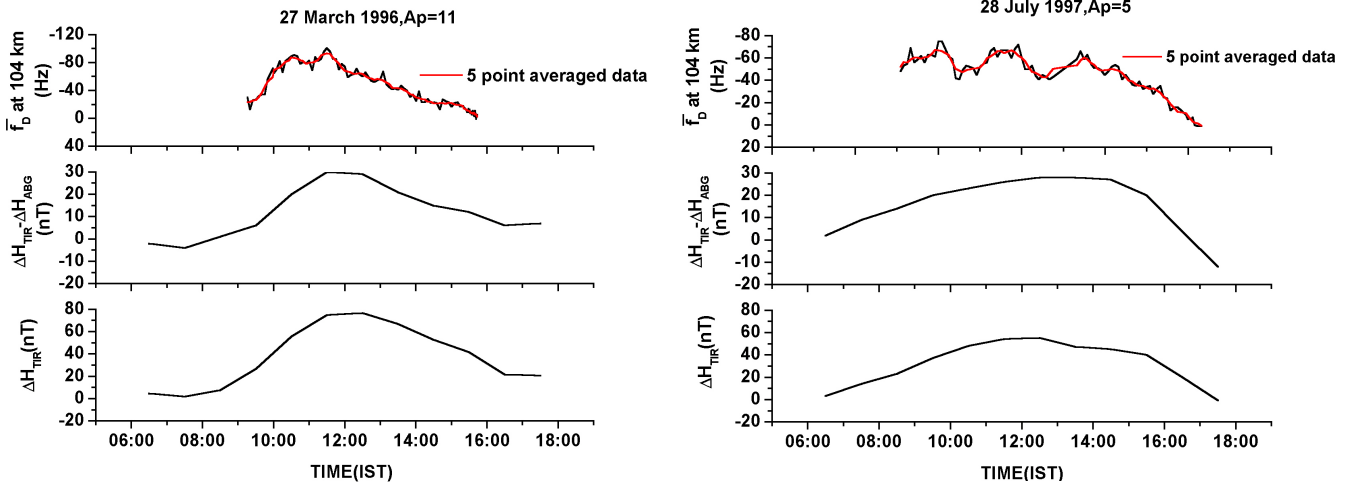


**Fig. 1.** VHF radar measured Doppler frequency ( $\bar{f}_D$ ) values in the EEJ corresponding to 104 km on a typical day (27 March 1996) during equinoctial period and a typical day (28 July 1997) during solstitial period along with the  $\Delta H_{TIR}$  and  $\Delta H_{TIR} - \Delta H_{ABG}$  values corresponding to the same days.

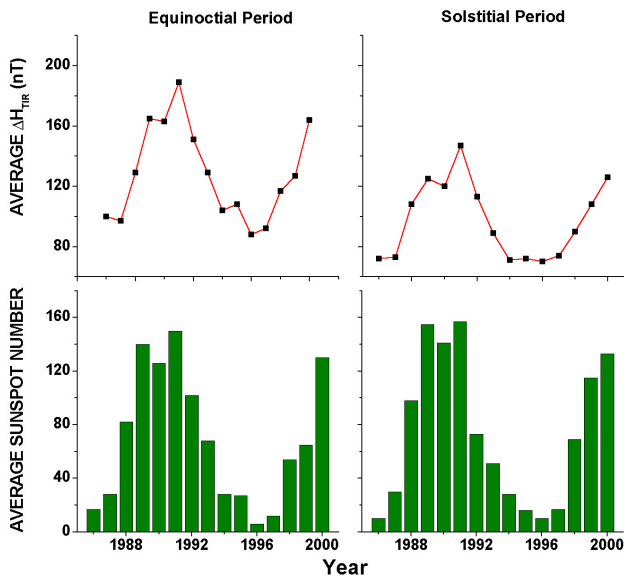


**Fig. 2.** Variations in the average noontime values of  $\Delta H_{TIR}$  with the average values of sunspot numbers for the equinoctial and the solstitial months during 1986–2000. Magnetically quiet days with  $A_p \leq 15$  only are included.

dependence also have a control on the occurrence of both CEJ and  $E_{sb}$ .

As a systematic measurement of the east-west electric field in the EEJ region at Trivandrum using the VHF radar is rather sparse, we have used the value of  $\Delta H_{TIR}$  around noontime as a proxy parameter representing the noontime east-west electric field in the EEJ region (Anderson et al., 2002). This approach is based on the known relationship between  $\Delta H$

values and the east west current intensity ( $J$ ) in the EEJ region and thereby to the east-west electric field ( $E_y$ ). In this context we have made a comparative study of the variation of the noontime values of  $\Delta H_{TIR}$  with the corresponding values of ( $\bar{f}_D$ ) during the equinoctial and solstitial periods.

Figure 1 shows a comparison of the VHF radar measured ( $\bar{f}_D$ ) values (proportional to  $E_y$ ) corresponding to the peak height (104 km) of the daytime electrojet on two typical days, namely 27 March 1996 and 28 July 1997 (as representative of the equinoctial and solstitial periods of the solar minimum years) with the  $\Delta H_{TIR}$  and  $\Delta H_{TIR} - \Delta H_{ABG}$  values corresponding to the same days. The nearly in phase variation of  $\Delta H_{TIR}$  and ( $\bar{f}_D$ ) from the VHF radar observations validate the use of  $\Delta H_{TIR}$  as a proxy parameter to represent the east-west electric field in the EEJ region. A similar in phase variation is manifested by  $\Delta H_{TIR} - \Delta H_{ABG}$  also although its values are less than that of  $\Delta H_{TIR}$ . The availability of the VHF radar data only for the period 1995–2000 is one serious limitation for the determination of the electric field from the VHF radar data for the entire period of study (1986–2000) and hence we have used the parameter  $\Delta H_{TIR}$  instead. Following the above approach, Fig. 2 shows the variations in average noontime values of  $\Delta H_{TIR}$  and average values of the sunspot numbers ( $S$ ) for the equinoctial period and solstitial period of each year of 1986–2000. A comparison of the solar cycle variations during the equinoctial and solstitial periods shows a close similarity between them except for the considerable differences in their average values during each year of the cycle, which are considerably lower during the solstitial periods in comparison to the equinoctial periods. This is an important characteristic of the noontime average electric field in the EEJ during the equinoctial and solstitial periods as the solar cycle changes from minimum to maximum

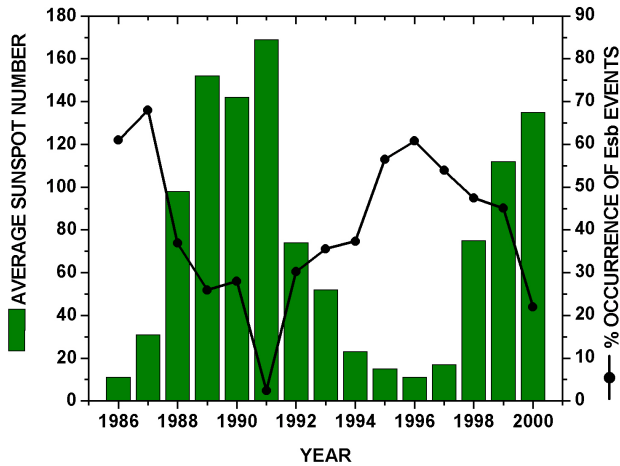


**Fig. 3a.** Distribution of the percentage occurrence of the  $E_{sb}$  events on days with  $A_p < 15$ , during the solstitial months with the average sunspot numbers corresponding to these days of the months of each year from 1986–2000.

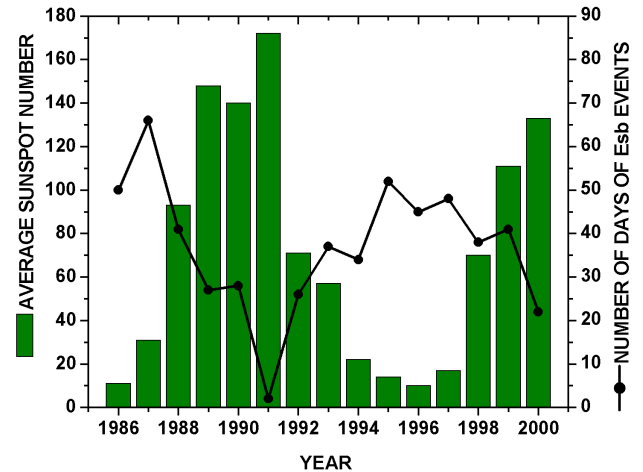


**Fig. 3b.** Distribution of the total number of occurrence of the  $E_{sb}$  events during the solstitial months with the average sunspot numbers corresponding to these days of the months of each year from 1986–2000. Magnetically quiet days with  $A_p \leq 15$  are included in the distribution.

phase. These variations also show that the noontime electric field values (as inferred from the above figure) during the solstitial periods are about 79% of the equinoctial period electric field values during the solar maximum years, while in the case of solar minimum years, the above values are of the order of 55% only. This shows that the effect of solar cycle changes on the electric field variations during equinoctial periods and solstitial periods are distinctly different. Such a significant reduction in noontime electric field during the solstitial months of the solar minimum periods results in low values of current in the EEJ region during the afternoon hours, providing a favorable background condition for the occurrence of CEJ and formation of blanketing  $E_s$  layers (Reddy and Devasia, 1977). In this study, we have also brought out the solar activity control of the reduction of noontime electric field in the EEJ region during solstitial period, which explains the variation in the blanketing  $E_s$  occurrence characteristics during the period from year to year.

### 3.2 Statistics of occurrence of blanketing $E_s$ and its related features over a solar cycle

The occurrence of blanketing  $E_s$  at Trivandrum was reported to have a strong seasonal dependence with the maximum number of days of occurrence confined to the solstitial months of May, June, July and August (Devasia, 1976) which was essentially based on the ionograms of Trivandrum for the solar quiet periods of 1969–1972. The present study indicates that even during the solstitial period, the characteristics of their occurrence vary from year to year depending on the solar cycle phase. Some of the important characteristics of the blanketing  $E_s$  events that have been studied in greater detail in the present investigation are: (i) the number of occurrence

of  $E_{sb}$  during each year (ii) the onset time of  $E_{sb}$  events; (iii) the nature of the background east-west electric field and its variability just before the onset of each  $E_{sb}$  event. We have examined these characteristics pertaining to the  $E_{sb}$  events for the period of 1986–2000 and some of the related aspects are discussed below in detail.

To illustrate the solar cycle dependence of the occurrence of  $E_{sb}$ , we are showing in Fig. 3a the distribution of the percentage occurrence of  $E_{sb}$  events during May, June, July and August months of each year against the average sunspot number for these months of each year. The figure shows a strong solar activity control on the occurrence of  $E_{sb}$  events, with the occurrence percentage as large as 70% during solar minimum years to as low as 5% in the solar maximum years. The occurrence of  $E_{sb}$  on days with  $A_p < 15$  only has been considered in order to study their behaviour on magnetically quiet days and hence Fig. 3b illustrates a distribution of such events during solstitial period of each year against the average sunspot number for the same days of the solstitial period of the same years. There is not much of a significant difference between the two distributions except for the small noticeable differences during the solar minimum epoch of 1994–1997. This is because of a natural consequence that the solstitial months of low solar activity periods have  $E_{sb}$  occurrences even on days with  $A_p > 15$ , whereas during high solar activity periods, the occurrence of  $E_{sb}$  events are mostly restricted to magnetically quiet days only.

#### 3.2.1 $E_{sb}$ events: some illustrative examples

During the solstitial period of each year of the solar cycle period under consideration, we have selected certain

magnetically quiet days with  $A_p < 10$  for the purpose of illustrating the varying nature of occurrence of blanketing  $E_s$  using sample ionograms corresponding to the onset, maximum and decay phases of the blanketing  $E_s$  layers. Figure 4 shows a few illustrative cases of occurrence of  $E_{sb}$  events during different phases of the solar cycle. All these events are associated with the occurrence of CEJ events with varying degrees of intensity as indicated by the variations in  $\Delta H_{TIR} - \Delta H_{ABG}$ . These illustrative cases of  $E_{sb}$  events show significant variabilities in their onset time, intensity and time of maximum intensity as well as in their duration. The maximum values of  $\Delta H_{TIR}$  (around noon time) corresponding to each of these events also show significant variabilities as each one of these events correspond to different phases of the solar cycle.

### 3.2.2 Noontime electrodynamic conditions of the EEJ and their control on the occurrence of $E_{sb}$ layers

It is fairly well known that the electrodynamic processes in the EEJ region on magnetically quiet days are mostly controlled by electric fields which are mainly due to (i) the global scale dynamo electric field ( $E_y$ ) and the resulting polarization electric field ( $E_p$ ) which drives the EEJ and (ii) the wind generated electric field ( $E_w$ ) due to the local interaction of height-varying winds with the electrojet plasma. It is the net polarization electric field due to both  $E_y$  and  $E_w$  that is controlling the basic electrodynamic of the EEJ region. As already mentioned, we have used the average of the noontime maximum values of  $\Delta H_{TIR}$  during the May, June, July, August months to arrive at an estimate of the noontime average electric field during each year corresponding to this season. In the present analysis, we have used data corresponding to the magnetically quiet days with  $A_p < 15$ . Figure 5 illustrates the nature of dependence between the number of days of  $E_{sb}$  occurrence during these months and the average noontime maximum values of  $\Delta H_{TIR}$  during these months of each year. The figure also shows the nature of solar cycle variation of the noontime electric field during the solstitial period of 1986–2000. The figure indicates a strong negative correlation between the two parameters which clearly brings out the fact that even during the solstitial months large electric fields in the EEJ region tend to inhibit the occurrence of CEJ and associated  $E_{sb}$  layers, which is obviously the case during solar maximum periods with the number of days of occurrence of  $E_{sb}$  events being very low and that too on magnetically quiet days only. The figure also indicates a critical value of about 120 nT for the average noontime maximum value for  $\Delta H_{TIR}$  during the solstitial period above which the number of days of  $E_{sb}$  events drastically decreases to a very low value. This is particularly noticeable in the case of the solar maximum year of 1991 where  $\Delta H_{TIR} \gg 120$  nT and the number of days of  $E_{sb}$  occurrence is just two only. Referring back to Fig. 2, it is interesting to note that the average noontime values of  $\Delta H_{TIR}$  during the equinoctial period

(March–April months) of many of the years covering the solar maximum phases during 1986–2000 are above 120 nT. Even during other years, though the  $\Delta H_{TIR}$  values during the equinoctial periods are less than 120 nT (average value also being  $\approx 120$  nT) they are much above the corresponding year's average level of  $\approx 90$  nT for the solstitial periods. Thus it appears as if there is a significant role for a larger noontime electric field in inhibiting the physical processes leading to the occurrence of CEJ and  $E_{sb}$  events even during the solstitial months of the different phases of the solar cycle. The year to year variability in the occurrence of CEJ events and associated blanketing  $E_s$  events thus seems to be strongly controlled by the ambient noontime electrodynamic which itself has substantial solar activity related variabilities from year to year.

### 3.2.3 Onset time of $E_{sb}$ events

As the occurrence of  $E_{sb}$  events is found to be mostly associated with the occurrence of CEJ events during the solstitial period, it is natural to expect the onset phases of the  $E_{sb}$  events and the CEJ events to coincide on a case-by-case basis. A careful analysis of each  $E_{sb}$  event during different years of the solar cycle have indicated certain interesting aspects of onset, growth and decay phases of the  $E_{sb}$  events in the presence of CEJ events of varying intensity and duration. Figure 6 shows the distribution of the most probable times of onset of blanketing  $E_s$  events during the solstitial period (middle panel) along with the average value of sunspot number for the same period of each year (bottom panel). The figure shows an important aspect of the solar cycle dependence of the onset times of blanketing  $E_s$  as revealed by the variations of the average sun spot number during 1986–2000. It is found that during solar minimum periods, the occurrence of  $E_{sb}$  events are confined mostly to the afternoon hours, with the times of occurrence becoming later and later to the evening hours as the solar maximum period is approached.

### 3.2.4 E-region electric field gradient in the afternoon hours before the onset of $E_{sb}$

In order to understand the effect of decreasing noontime maximum electric field (as indicated by  $\Delta H_{TIR}$ ) in the EEJ region leading to CEJ and thereby on the onset timings of  $E_{sb}$  events, these events have been examined in relation to the average gradient of the electric fields that are present before the onset of the CEJ event. The electric field gradient in the present context is given by the time rate of change of the difference between the  $\Delta H_{TIR}$  value just before the onset of the CEJ event and the noontime maximum value of  $\Delta H_{TIR}$ . The average gradient thus obtained is shown in the top panel of Fig. 6 which also shows clear solar activity dependence. The implication of this is that the solar minimum periods are associated with a more or less slow and gradual decrease of the noontime maximum electric field whereas the

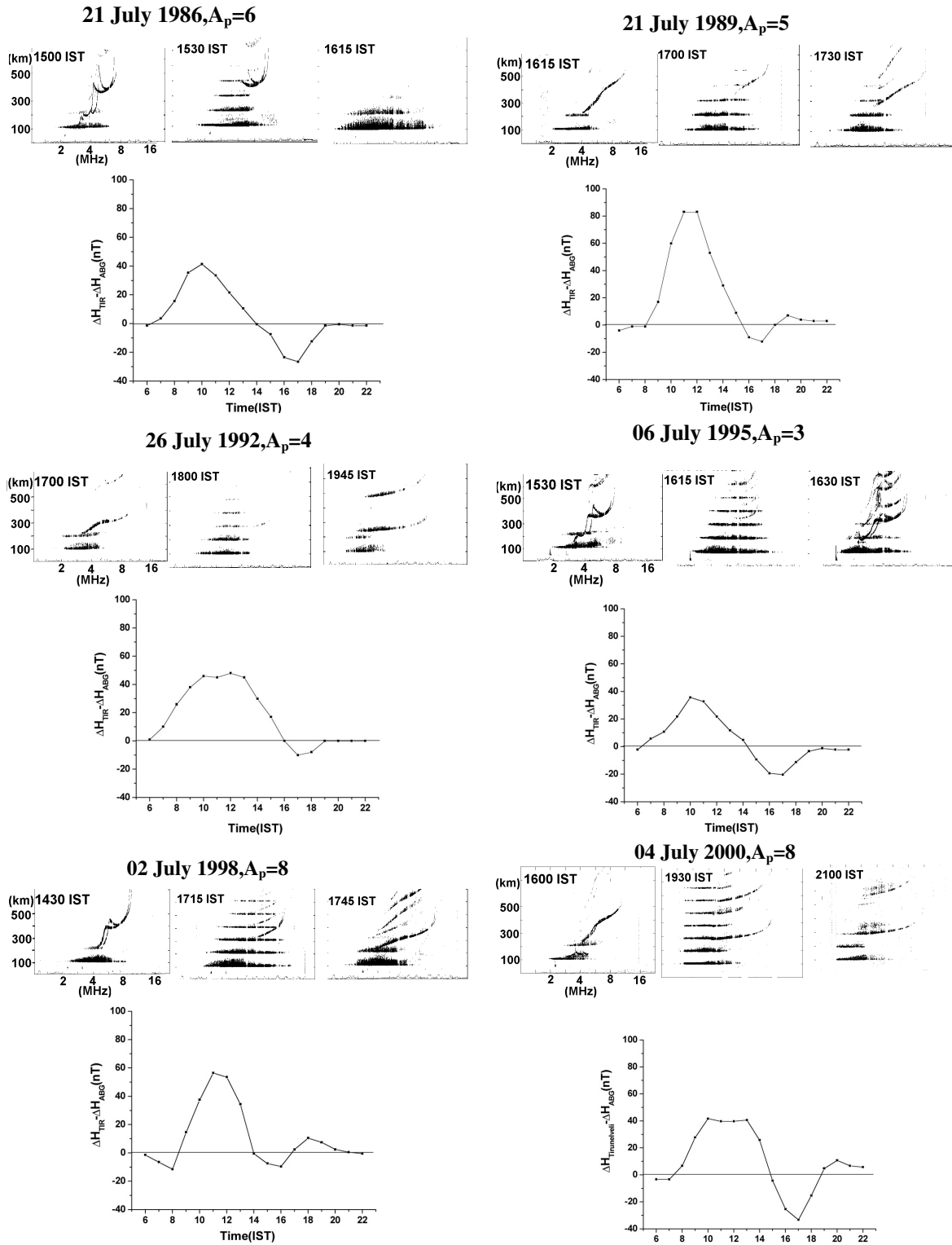


**Fig. 4.** Some illustrative cases of  $E_{sb}$  events during different phases of the solar cycle. Events occurring only on very magnetically quiet days with  $A_p \leq 10$  are included.

**Table 1.** The number of days of  $E_{sb}$  events during the solstitial months of 1986–2000 and their average characteristics.

Year	Average Sunspot number	Number of days of $E_{sb}$ events	Average Onset time (h)	Average noontime $\Delta H_{TIR}$ (nT)	Average Gradient (nT/h)
1986	11	50	15:59	68	-14
1987	31	66	15:50	71	-15
1988	93	41	16:39	100	-20
1989	148	27	16:52	120	-22
1990	140	28	16:22	115	-22
1991	172	2	17:00	162	-30
1992	71	26	16:44	109	-20
1993	57	37	16:19	88	-17
1994	22	34	16:39	72	-16
1995	14	52	15:35	72	-17
1996	10	45	16:09	68	-13
1997	17	48	16:02	74	-16
1998	70	38	16:08	90	-17
1999	111	41	16:24	108	-20
2000	133	22	16:35	116	-22

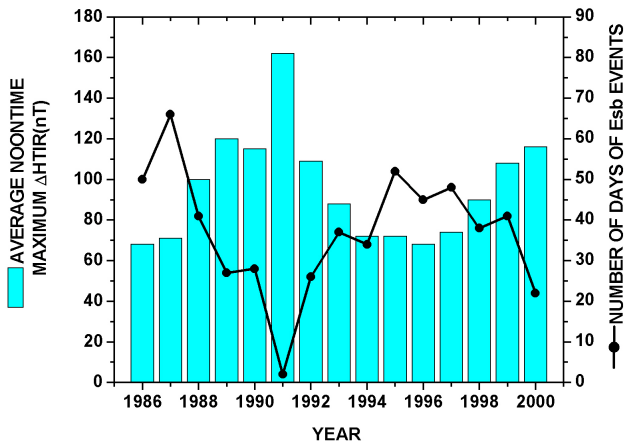


**Fig. 5.** Variation in the number of  $E_{sb}$  events during the solstitial months with the average noontime maximum  $\Delta H_{TIR}$  during those days (with  $A_p \leq 15$ ).

solar maximum periods show a steep and somewhat faster decrease of the noon time electric field towards evening hours as the onset time of the CEJ events themselves are getting time shifted towards evening hours. The effect of these varying gradients in the noontime electric fields (equivalently in  $\Delta H_{TIR}$ ) on the occurrence of blanketing  $E_s$  events is that during solar minimum periods, the slow and gradual decrease of the noontime  $\Delta H_{TIR}$  results in a CEJ event with a comparatively lower intensity. This in turn implies the presence of a low value of westward electric field, which is considered as favorable for the occurrence of  $E_{sb}$  event and its sustenance. In the case of solar maximum periods, the sharp

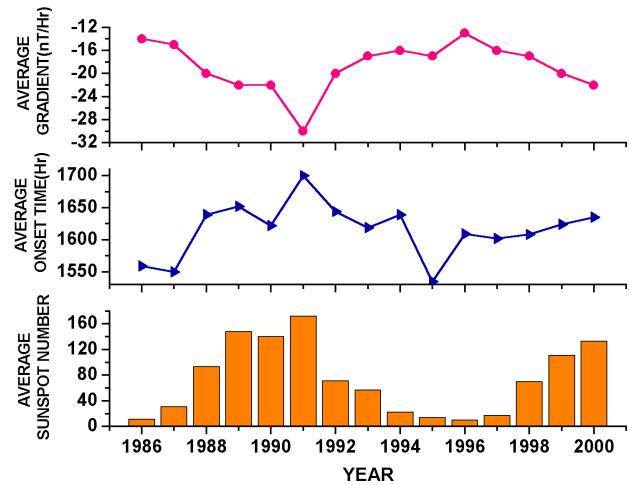


**Fig. 6.** Top panel: Distribution of the most probable values of the average gradient of the magnetic field ( $\Delta H$ ) associated with  $E_{sb}$  events of each year with the average sunspot numbers for the same days of each year. Bottom panel: Distribution of the most probable onset time of the  $E_{sb}$  events with the average sunspot numbers for the same days of each year.

decrease from comparatively larger noontime  $\Delta H_{TIR}$  values results in CEJ events with larger intensity (larger westward electric field), which is not very favorable for the occurrence of an  $E_{sb}$  event.

From the above discussions, it is very much relevant to put all the observed characteristics of the  $E_{sb}$  events during 1986–2000 in the form of a table. Table 1 indicates the number of days of  $E_{sb}$  events during the solstitial months

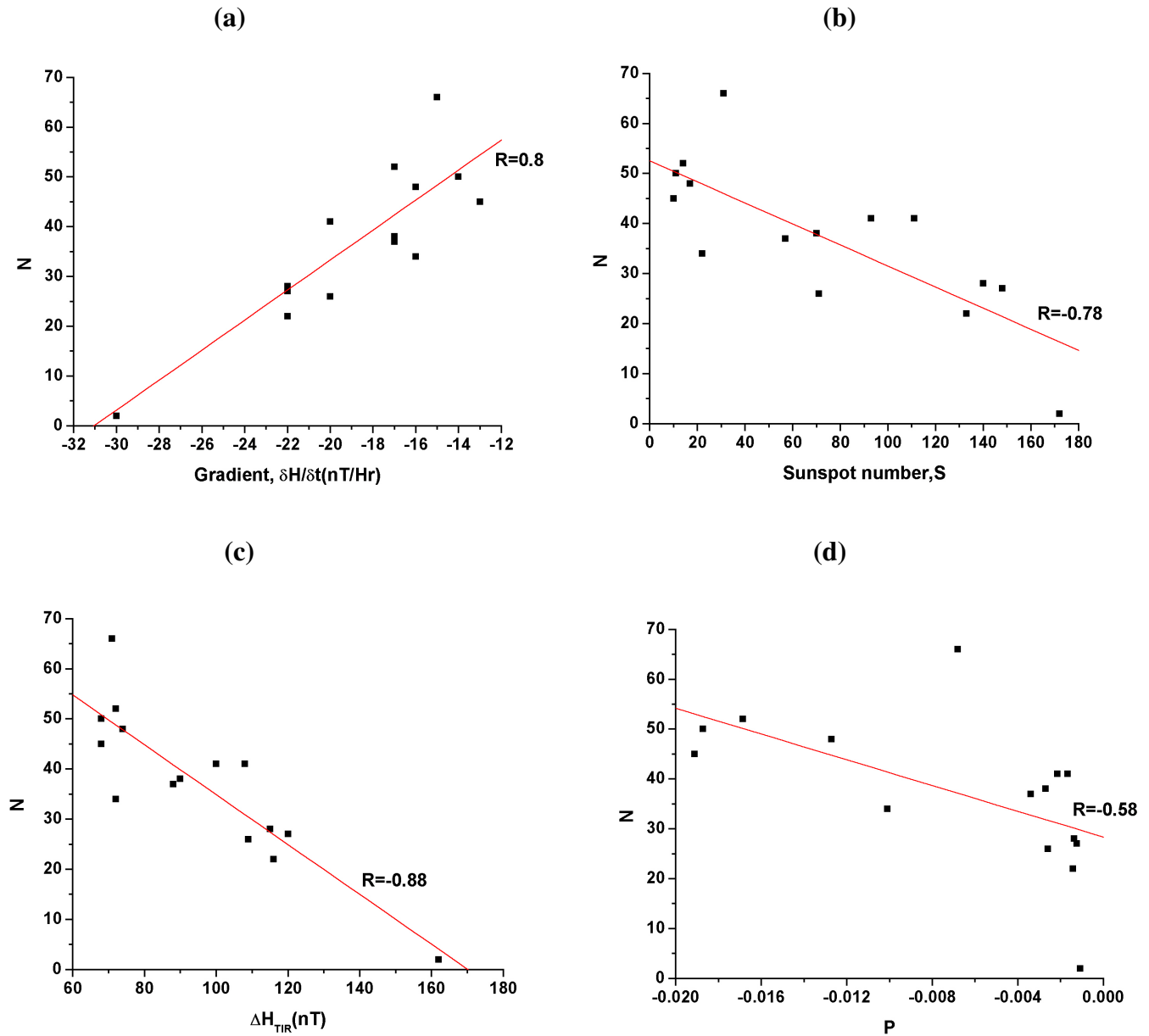


**Fig. 7.** Graphical representation of the relationship between the number of days of  $E_{sb}$  events ( $N$ ) and (a) average gradient,  $\frac{\delta H}{\delta t}$ , (b) average sunspot number,  $S$ , (c) average noontime maximum  $\Delta H_{TIR}$ , (d) the factor  $P$  for each year during 1986–2000.

of each year against their average onset times. The average noontime  $\Delta H_{TIR}$  and its average gradient before the onset of  $E_{sb}$  are also shown in the table. It is also clear from the table that the maximum number of days of  $E_{sb}$  occurrence was during 1987 (66 days) and during 1995 (52 days) with a deep minimum with just only 2 days of occurrence during 1991. Interestingly, the year 1991 was also characterized by a significantly larger noontime value of  $\Delta H_{TIR}=162$  nT and a very large negative gradient ( $-30$  nT/Hr) whereas the years 1987 and 1995 have almost identical low values for the average  $\Delta H_{TIR}$  (71 nT and 72 nT) and average gradient ( $-15$  nT/Hr and  $-17$  nT/Hr). The table also indicates the

nature of relationship between the number of days of  $E_{sb}$  events ( $N$ ), and average values of sunspot number ( $S$ ), average values of  $\Delta H_{TIR}$  and average values of electric field gradient ( $\delta H/\delta t$ ) during each year of the solar cycle. Figure 7 illustrates the correlation between the number of days of blanketing  $E_s$  ( $N$ ) against each of these parameters. The correlation coefficients between the number of days of blanketing  $E_s$  ( $N$ ) against each of these parameters are found to be reasonably high between 0.7–0.8 in each case. As  $N$  is well correlated with each of these parameters, we can put them as:

$$N \propto \delta H / \delta t \quad (2)$$

$$N \propto 1/S \quad (3)$$

$$N \propto 1/\Delta H_{TIR} \quad (4)$$

These proportionalities have enabled us to represent the number of days of  $E_{sb}$  events ( $N$ ) as a function of the combined effect of average sunspot number ( $S$ ), average noontime maximum  $\Delta H_{TIR}$  and the average gradient  $\delta H/\delta t$ , by the functional relationship of the form:

$$N \propto P \quad (5)$$

where

$$P \propto (\delta H/\delta t)/(S\Delta H_{TIR}) \quad (6)$$

A graphical representation of this functional relationship between  $P$  and the number of days of  $E_{sb}$  events ( $N$ ) is shown for the period 1986–2000 in Fig. 7. The graph shows a linear relationship between total effectiveness of all the parameters as represented by  $P$  and the number of  $E_{sb}$  days with a very good correlation coefficient. This linear relationship, though based on average values of all the related parameters is not expected to vary too much on a day-to-day basis during the solstitial period of each year. Hence this provides a simple method of predicting the occurrence probability of blanketing  $E_s$  on a day to day basis during the solstitial months using the average representative values of sunspot number, noontime  $\Delta H_{TIR}$  and the afternoon gradient of the decrease of  $\Delta H_{TIR}$ .

### 3.3 Physical significance of blanketing frequency of $E_s$ layers ( $f_b E_s$ )

As mentioned earlier, the blanketing frequency of the  $E_s$  layer ( $f_b E_s$ ) represents the maximum frequency of the layer at which the E-layer starts becoming transparent. It was a common practice in the past to make ionosonde observations on  $E_s$  almost simultaneously with the rocket measurements of its electron density profiles. Reviewing such measurements, Smith (1966) has pointed out that blanketing frequency ( $f_b E_s$ ), corresponds generally to the rocket measured maximum plasma frequency in the E-layer, so that  $f_b E_s$  can be taken as giving a direct measurement of the maximum electron concentration in the  $E_s$  layers. This maximum electron concentration ( $N_{max}$ ) is related to the maximum plasma frequency of the layer through the equation

$$f_{N_{max}}^2 = 0.801 N_{max} 10^6 \quad (7)$$

The electron concentration as deduced from  $f_b E_s$  value is found to agree with the rocket measured maximum electron concentration in the  $E_s$  layer with deviations of about 10% on the average. This brings into focus the physical significance of  $f_b E_s$  variations in the background E-region behavior. Figure 8a represents the time variation of  $f_b E_s$  corresponding to

some representative  $E_{sb}$  events during the solstitial period of each year during 1986–2000. Typical long duration events with multiple reflections which is characteristic of the intensity of the  $E_{sb}$  layer formed have been selected as illustrative cases. As it is clear from the figure, the onset time of the events in the afternoon hours as well as their duration are varying considerably over the solar cycle period of 1986–2000. The duration of the events varies in general from 2–5 h. The beginning phase of the events is in general associated with larger values of  $f_b E_s$  and their height locations shown in Fig. 8b are also well above 100 km where the normal daytime  $E_s$  layer is formed. The decay of the blanketing  $E_s$  layer with time is manifested by a gradual decrease in  $f_b E_s$  values and their corresponding height locations also show a gradual fall even going below the 100 km level. This is an important feature of the formation and decay of the  $E_{sb}$  layer suggesting the role of descending wind shear mode of tidal/gravity wave winds in the E-region interacting with the electrojet plasma. It may be mentioned that larger values of  $f_b E_s$  at the onset and growth phases of an  $E_{sb}$  layer are indicative of the presence of very sharp electron density gradients of the  $E_{sb}$  layer (Reddy and Devasia, 1977), which can give a large growth rate to the plasma instabilities even in the presence of a very weak electric field. The variations of  $f_b E_s$  with time as well as the height locations of the  $E_{sb}$  layer in the EEJ region have important roles in the growth and sustenance of gradient instabilities during Counter Electrojet events when the east-west electric field is very weak (Devasia et al., 2004).

### 3.4 VHF radar observations of blanketing $E_s$ layers and associated irregularities

The 54.95 MHz VHF radar observations of the EEJ irregularities at Trivandrum on several occasions during the period of 1995–2000 have shown that the drift velocities of the day time  $E_s$  irregularities are in general small in the late afternoon hours (in comparison to the midday values). So under this condition gradient instabilities of 2.7 m scale-size cannot be sustained with the normal E-region electron density gradients and the small electric fields present at this time (Reddy and Devasia, 1977). Whereas during solstitial months the appearance of a CEJ event and associated blanketing  $E_s$  layer during the weakened EEJ condition (or CEJ) in the afternoon hours provided the necessary condition of electron density gradients in the right direction so as to generate gradient drift instabilities. Radar observations of many such events of blanketing type  $E_s$  layer occurrences during the solstitial months have shown that such layer type  $E_{sb}$  irregularities in the EEJ region give rise to strong backscattering of 54.95 MHz radar signals (Reddy and Devasia, 1977; Devasia et al., 2004). Remarkable changes in the amplitude and Doppler frequency spectra of the radar backscattered signals were observed coinciding with the appearance of blanketing  $E_s$  layers in the ionograms simultaneously obtained from the colocated ionosonde at Trivandrum. VHF radar observations

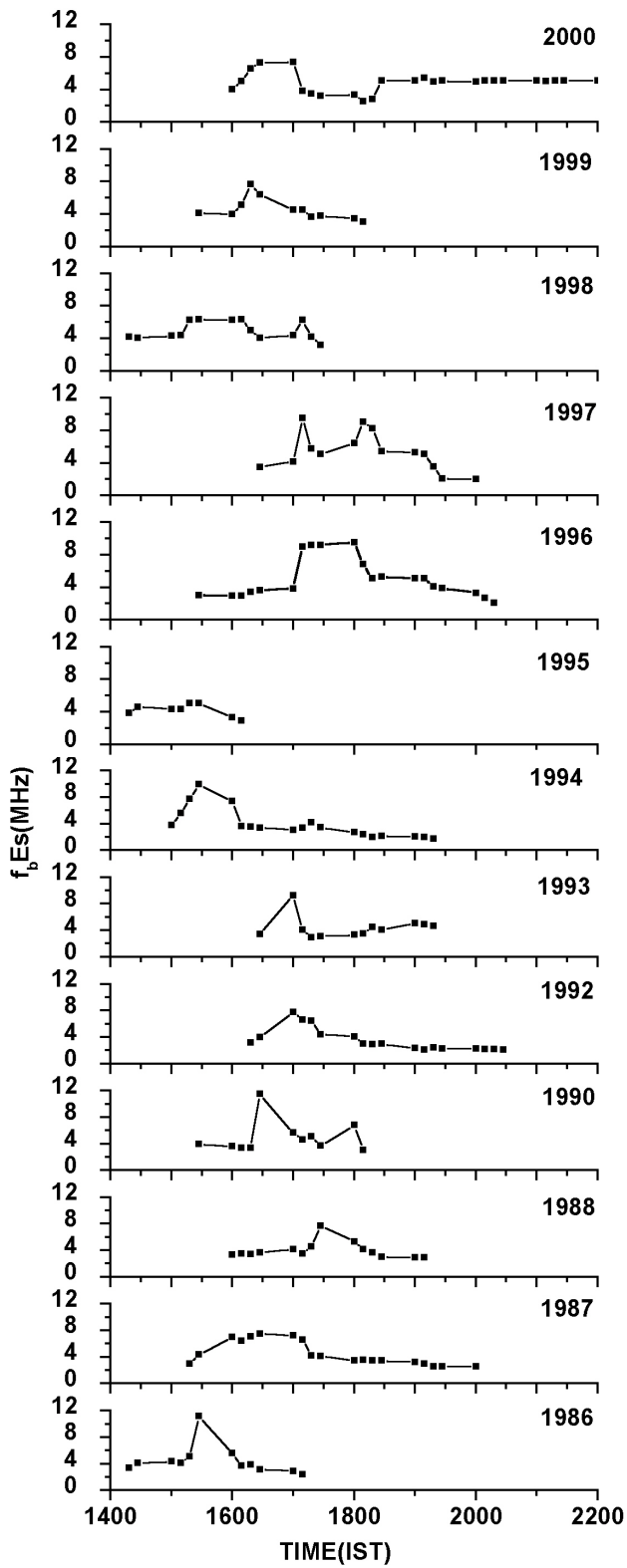


**Fig. 8a.** Time variation of  $f_b E_s$  corresponding to some strong  $E_{sb}$  events during 1986–2000.

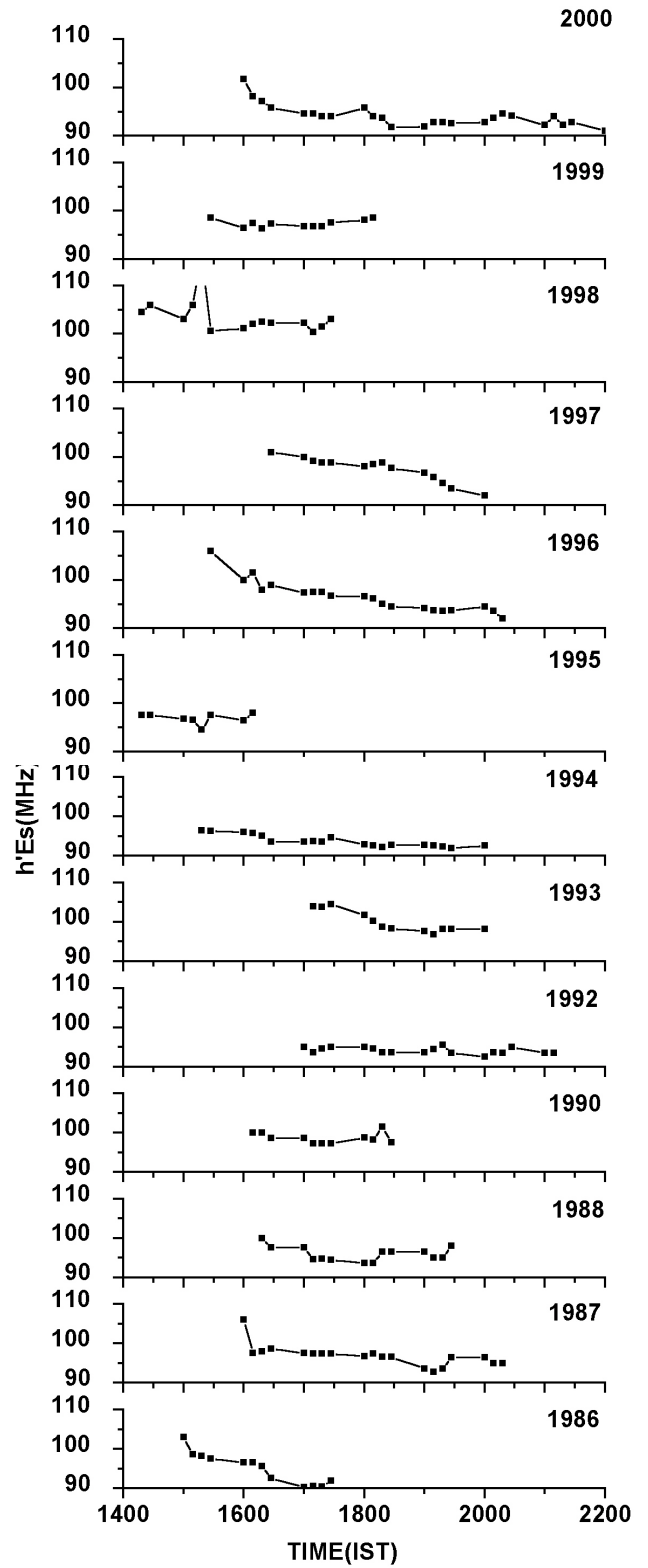


**Fig. 8b.** Time variation of  $h' E_s$  corresponding to the same  $E_{sb}$  events.

thus have been highly useful in interpreting the observed characteristics of blanketing  $E_s$  layers in terms of their implications in the generation and decay processes of gradient instabilities during CEJ events.

In this context we have made a few case studies of radar observations on  $E_{sb}$  layers with a view to understand the relative roles of the vertical electric field and the vertical electron density gradient in the sustenance of gradient instabilities during different phases of the solar cycle using the available radar data. These radar observations have shown that in all the cases the initial formation of the blanketing  $E_s$  layers takes place only at such times when the drift velocities of the EEJ irregularities are small. The distinct features of the radar returns corresponding to certain blanketing  $E_s$  events which occurred at different phases of the solar cycle are presented here in order to bring out the solar activity control on them.

### 3.4.1 VHF radar backscattered signal characteristics during blanketing $E_s$ events

The most striking feature of the VHF radar observations from many of the blanketing  $E_s$  events is the sudden build up of the backscatter signal strength to larger values even exceeding the noontime values of radar returns from the normal  $E_s$  irregularities in the presence of a large east-west electric field. Such large signal returns from the blanketing  $E_s$  irregularities are associated with the large growth rate of the gradient instabilities mainly due to extremely sharp gradients of the  $E_{sb}$  layer even though the electric field is very low at this time (Devasia et al., 2004).

### 3.4.2 Illustrative cases of radar observations during different phases of the solar cycle

#### Case I: 30 July 1997 ( $A_p=7$ )

Figure 9a represents the VHF radar observed variations of mean Doppler velocity of irregularities corresponding to different height regions of the EEJ along with the variations of  $\Delta H_{TIR} - \Delta H_{ABG}$  (representing the electrojet strength) in the afternoon hours from 14:00 h onwards on 30 July 1997, which was a magnetically quiet day with  $A_p=7$ . The sharp decrease of the electrojet strength in the afternoon hours preceding the CEJ during 15:30–20:00 h is very clear from the figure. From Figs. 3 and 5, it may be noted that the year 1997 is in low solar activity phase with the average sunspot number  $\sim 15$  and the average noontime magnetic field is also low  $\sim 70$  nT. The appearance of blanketing  $E_s$  event during the CEJ event is illustrated using sample ionograms shown in Fig. 9a. Prior to the appearance of the CEJ and blanketing  $E_s$ , the mean Doppler velocity profiles are characteristic of the weak afternoon EEJ conditions and they provide a comprehensive picture of the gradual changes in the afternoon electrodynamics associated with the changes from the EEJ conditions to CEJ conditions. With the appearance of

the blanketing  $E_s$ , the altitude profiles of the mean Doppler velocity become more and more structured in comparison to their smooth variations prior to the occurrence of CEJ as shown in Fig. 9a. The velocity profiles become more and more confined to a narrower region of the EEJ as signals are observed from the thin  $E_{sb}$  layer. Further the velocity of the type II irregularities during the  $E_{sb}$  event is also very low indicating the presence of very low vertical electric field (weakly positive in the present case) during this time. The maximum strength of the CEJ event is at about 17:00 h (with peak  $\sim -25$  nT) whereas the blanketing  $E_s$  on the ionograms during the CEJ time shows its maximum intensity with more number of multiple reflections and largest value of  $f_b E_s$  (around 4.5 MHz) at around 16:20 h much before the time of CEJ peak. This also corresponds to the time of largest backscatter signals from the persisting  $E_{sb}$  layer.

The time variation of  $P_{max}$  (maximum backscattered power) is shown in Fig. 9b along with its corresponding variations in Doppler velocity and height locations. The mean Doppler velocity during this period is mostly negative indicating the presence of very low vertical electric field in the upward direction. This indicates the important role of very sharp electron density gradients of the  $E_{sb}$  layer in association with a very weak vertical electric field, in the large growth of gradient instabilities resulting in very strong backscattered echoes as shown in Fig. 9b. This is a unique situation in which the electron density gradients in the blanketing  $E_s$  layer has a more dominant role over the vertical polarization electric field in producing strong backscattered returns from the  $E_{sb}$  irregularities during the CEJ event. Beyond 16:20 h, the  $E_{sb}$  layer appears to weaken even though the CEJ intensity is further increasing till 17:00 h. This probably indicates even of a threshold level for the CEJ intensity at which the  $E_{sb}$  layer attains the maximum intensity. Further, it may also be noted from Fig. 3 that during the year 1997 more number of blanketing  $E_s$  events have been observed with the background conditions being governed by comparatively lower values of the vertical polarization electric field.

#### Case II: 4 July 2000 ( $A_p=8$ )

The radar observations of  $E_{sb}$  on this day is significantly different from the earlier event of 1997. The average sunspot number of the year is about 130 in comparison to the very low average of  $\sim 15$  during 1997 and the average noontime  $\Delta H_{TIR} \sim 115$  nT against the value of  $\Delta H_{TIR} \sim 70$  nT in 1997. This event is unique in several other aspects also. The day is characterized by the presence of a very strong CEJ event (peak  $\sim 45$  nT) during 14:45–18:30 h. Other noticeable features are the appearance of very strong  $E_{sb}$  with several multiple reflections (sometimes even blanketing the F-layer completely) in the ionograms corresponding to the peak time of CEJ almost close to 17:00 h and the presence of very strong backscattered radar returns. In this case also the large

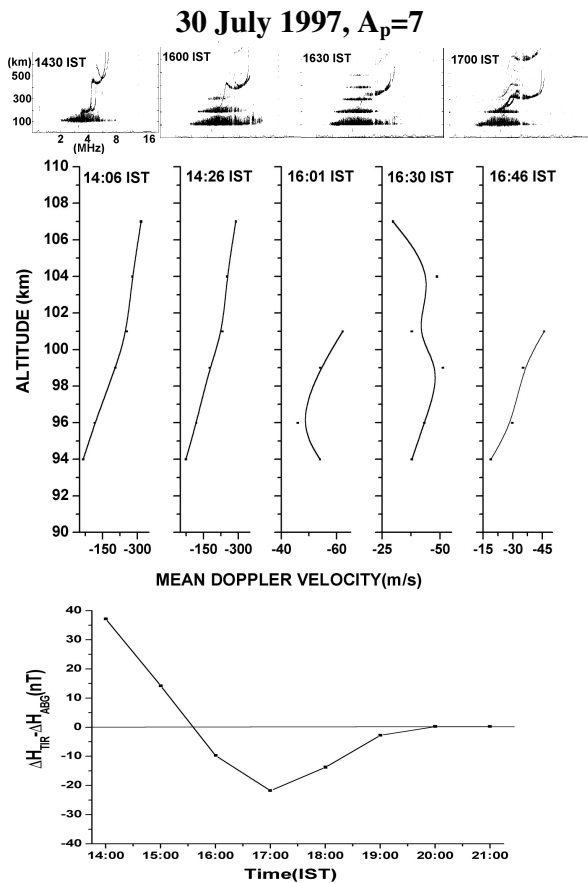


**Fig. 9a.** Height profiles of the VHF radar measured  $V_p$  values at selected times on 30 July 1997 (middle panel) with the representative ionograms during this time. The strength of the equatorial electrojet during 14:00–21:00 h is also shown in the figure (bottom panel).

growth of the gradient instabilities reached its maximum at  $\sim 16:20$  h with very strong radar returns even before the CEJ peak at 17:00 h. The height structure of the Doppler velocity profiles during the CEJ time showed large fluctuations and their main features are very clear from Fig. 10a. The figure also shows some of the ionograms corresponding to the peak time of the CEJ event between 16:55–17:30 h and the velocity profiles during this time show altitude variations with positive values of velocity below the peak height of the EEJ ( $\sim 100$  km) and larger values of negative velocity above this height region. This probably indicates the varying nature of oppositely directed plasma density gradients in the top and bottom sides of the persisting  $E_{sb}$  layers. They have significant role in the large growth and decay of gradient instabilities during CEJ as shown by the very large build up of backscattered power returns followed by their fast decay going through cycles of increase and decrease as shown in Fig. 10b. The time variation of  $P_{max}$  (maximum backscattered power) is also shown in the figure along with

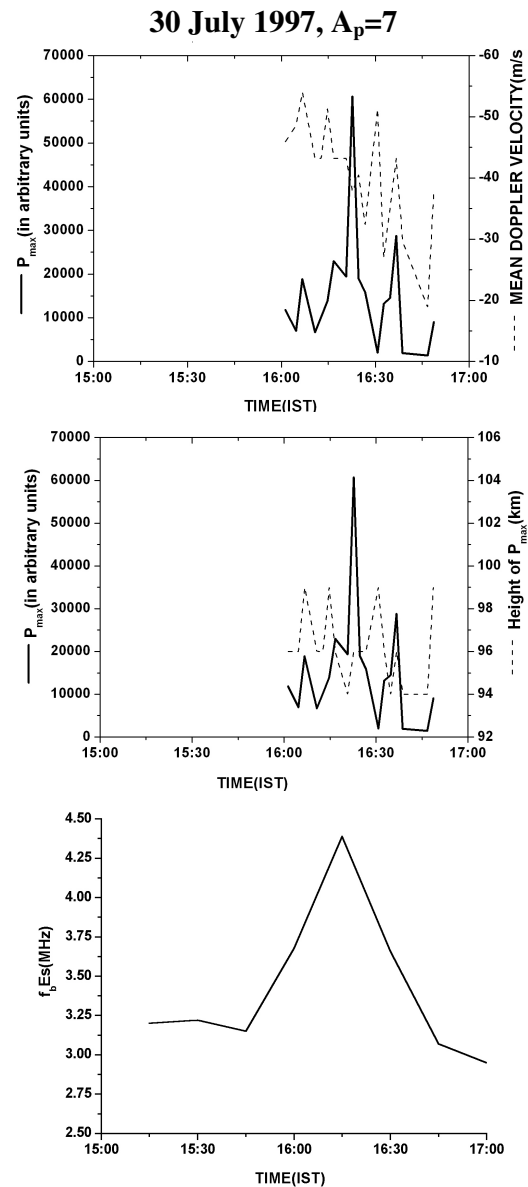


**Fig. 9b.** Time variation of the maximum backscattered power ( $P_{max}$ ) and the corresponding Doppler velocity values (top panel) during the  $E_{sb}$  event along with the variation of  $f_b E_s$  (bottom panel). Time variation of the maximum backscattered power ( $P_{max}$ ) and the corresponding height of scattering region (middle panel) is also shown.

its corresponding variations in Doppler velocity and height locations. The mean Doppler velocity during the initial phase is positive indicating the presence of a fairly large vertical electric field in the downward direction. The height location of  $P_{max}$  during this period is predominantly in the bottom gradient region. The strength of the maximum power return ( $P_{max}$ ) changes rapidly with time because of the fast changes in height location as well as in the gradient changes

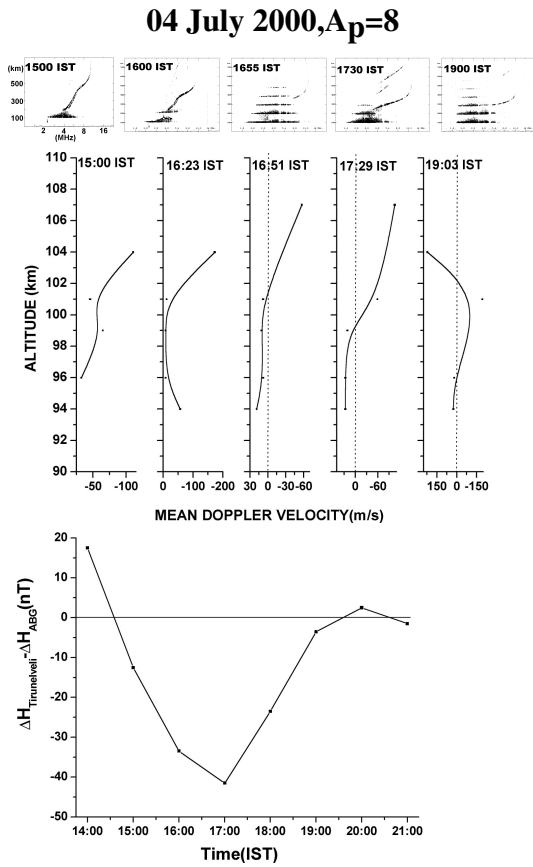


Fig. 10a. Same as Fig. 9a, but for 4 July 2000.

of the  $E_{sb}$  layer. The maximum value of  $f_b E_s$  on this day is about 7.5 MHz as shown in Fig. 10b and the  $P_{max}$  even exceeds much more than the level of maximum noontime power return on this day.

Because of the lack of radar observations covering different phases of the solar cycle, we have considered only two case studies belonging to two extreme conditions of sunspot activity – a minimum and a maximum.

#### 4 Discussion and conclusions

The main results of the present study may be summarized as:

1. The occurrence of blanketing  $E_s$  layers at the equatorial station of Trivandrum is observed frequently during the summer solstitial months of May, June, July and August and they occur mostly in association with the CEJ events that are characteristic of these months.
2. Even during these months their occurrences show very strong solar activity dependence with the occurrence frequency being very large during the solar minimum year and very low during solar maximum year. The

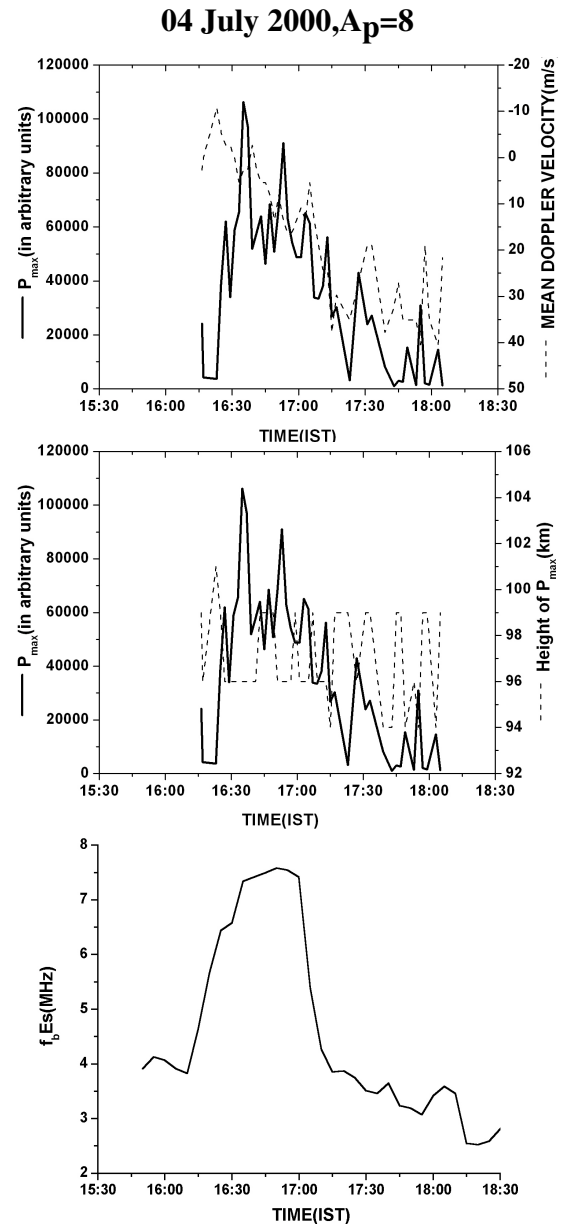


Fig. 10b. Same as Fig. 9b, but for 4 July 2000.

morphological characteristics of the  $E_{sb}$  layers-their onset time, intensity etc also show significant dependence on the solar activity level.

3. The onset time of the  $E_{sb}$  layers are mostly confined to the afternoon hours during solar minimum periods whereas it is confined more and more towards evening hours as the solar maximum periods are approached.
4. The more frequent occurrences of  $E_{sb}$  during the solar minimum periods are seen to be in association with CEJ events of lesser intensity, whereas the less frequent

occurrence of  $E_{sb}$  events during solar maximum periods are mostly in association with CEJ events of larger intensity.

5. The  $E_{sb}$  layers being thin layers of enhanced ionization with sharp electron density gradients on either side can give rise to very large growth of gradient instabilities in the electrojet plasma in combination with the vertical electric field of right magnitude and direction in the electrojet resulting in very strong radar backscattering. A change of direction of either the gradient or the electric field results in the decay or even disappearance of the gradient instabilities.
6. The relative effect of the magnitude and direction of the vertical electric field and the electron density gradient of the  $E_{sb}$  layer has a strong control in the generation of the plasma instability depending on the solar activity levels, with the gradient of the  $E_{sb}$  layer showing a dominant role during solar minimum and the electric field showing the dominant role during solar maximum conditions. These features are also in a way related to the competing influence of electric field and wind (through the generation of vertical polarization electric field by shearing winds) in the generation of  $E_{sb}$  layers.

The present studies have brought out some of the variabilities in the characteristic features of the post noon blanketing  $E_s$  layers over the magnetic equatorial location of Trivandrum during the summer solstitial months due to the solar activity changes. The ionosonde observations during this period show that the ionogram traces corresponding to  $E_{sq}$  and  $E_{sb}$  layers are distinctly different; with strong  $E_{sb}$  layers characterized by several multiple reflections and sometimes even totally blanketing the F-layer. It has been illustrated in the previous sections that the general characteristics of the  $E_{sb}$  layers—their onset time and duration, intensity as well as the strength of the CEJ events during which the  $E_{sb}$  layers are formed—are distinctly different during different years. Similar distinctly different characteristics are also manifested in the growth and sustenance of gradient instabilities during low and high solar activity periods as evidenced by the characteristics of the radar returns from the type II irregularities associated with the appearance of  $E_{sb}$  layers as revealed by the limited VHF radar data available. These distinctly different features are also shown in the height region of occurrence, signal strength and the Doppler spectral characteristics of the backscattered radar returns during the  $E_{sb}$  events.

Apart from the general characteristics of  $E_{sb}$  layers and that of VHF radar returns from them being different during solar minimum and maximum periods, certain other important aspects of the dominant physical processes controlling the growth processes of the gradient instabilities under varying solar activity conditions also appear to emerge from the present investigation. Some of the cases of radar returns from the  $E_{sb}$  layers that are illustrated in the previous sec-

tions show that the velocity profiles of the type II irregularities associated with  $E_{sb}$  layers show the presence of large velocity shears (Reddy and Devasia, 1981). As the occurrence of  $E_{sb}$  layers are in general associated with very weak (almost zero) east-west electric field, these velocity shears in the Doppler velocity profiles are equivalent to wind shears. The presence of an  $E_{sb}$  layer under the background conditions of a very weak east-west electric field and large shears in the Doppler velocity profiles of the type II irregularities associated with it suggest to the existence of highly structured wind-induced polarization electric field generated by the height varying zonal winds in the EEJ region (Reddy and Devasia, 1981). Some of the Doppler velocity profiles shown in the present studies have a close similarity to the reversal of drift velocity with height as shown by Reddy (1989). This is in sharp contrast with the nature of the Doppler velocity profiles from  $E_{sq}$  irregularities in the EEJ which in most cases resemble the smooth profile of the vertical polarization electric field ( $E_p$ ) due to  $E_y$  indicating the dominant role of the east-west electric field. Hence in studying the characteristics of Doppler velocity profiles associated with the  $E_{sq}$  irregularities during EEJ and those associated with the  $E_{sb}$  irregularities during CEJ, we have to consider the competing roles of electric field (through the vertical polarization field  $E_p$ ) and wind (through the wind generated polarization electric field,  $E_w$ ). Even while we are restricting our discussion to the  $E_{sb}$  events of different years of the solar cycle, the competing roles of the electric field and wind appear to control their characteristics like onset time, duration and even the intensity of the radar returns and its Doppler velocity from the  $E_{sb}$  layers. This feature is indicated by the relatively very low value of the electric field (eastward or equivalently vertical in the upward direction) during the time of onset of  $E_{sb}$ , its development into a very strong  $E_{sb}$  event with several multiple reflections as well as in the appearance of very sharp velocity shears in the Doppler velocity profiles of the large radar returns (which even exceeds the daytime maximum value) from such layers. All these features are mostly manifested by the  $E_{sb}$  events occurring quite frequently during solar minimum years. Whereas in the case of the very few events observed during the solar maximum years, their onset itself is under the background condition of a fairly significant westward electric field (i.e. vertical electric field in the downward direction) during the CEJ event. The strength of radar returns depend mainly on the proper combination of the magnitude and direction of both the electric field and the gradients. The altitude structures of the Doppler velocity profiles also depend mainly on the relative effect of the sharpness of the gradients in comparison to the electric field. All these features are manifested in the two cases cited in Figs. 9 and 10.

The competing roles of the electric field and wind induced shears in the velocity profiles of the type II irregularities from  $E_{sb}$  layers bring into focus the varied nature of their implications in the growth process of gradient drift instability

during different phases of the solar cycle. This aspect will be more clear considering the effects of the gradient term on the type II waves in the EEJ as have been explained by Farley and Balsley (1973) and Fejer et al. (1975). The growth rate of the gradient instability in the EEJ region (Fejer and Kelly, 1980) is controlled by the relative roles of the vertical polarization electric field and the vertical electron density gradient. In this context a comparative study on the occurrence features of  $E_{sb}$  layers with due consideration to their generation mechanism could lead to a better understanding of the competing roles of the equatorial electric fields and winds over a solar cycle. The results of a detailed analysis of sporadic E-layer occurrences over the equatorial station Fortaleza in Brazil for a period 15 years from 1975–1990 by Abdu et al. (1996) have shown the competing roles of the equatorial zonal electric field and wind systems as well as their long term changes in the generation of the different types of  $E_s$  layers. They have attributed the  $F_{10.7}$  cm radio flux variation during the solar cycle as controlling both the electric field and E-region winds in the equatorial region.

The description of the various forms of afternoon  $E_{sb}$  and its associated characteristics given in the previous sections brings into focus certain significant aspects of the growth and decay of the gradient instabilities in the presence of  $E_{sb}$  layers under conditions of weak/reversed electric field and very sharp and variable electron density gradients during solar minimum and maximum conditions. The relative role of the electric field is more significant during solar maximum conditions whereas during solar minimum conditions, the plasma instability growth conditions are more significantly controlled by the very sharp electron density gradients of the very intense  $E_{sb}$  layers which appear under conditions of near zero electric field.

The occurrence of  $E_{sb}$  in the early morning hours of 04:00–06:00 h has also been observed at Trivandrum coinciding with similar conditions of E region electric field existing at such times. In both the cases of  $E_{sb}$  occurrences during afternoon and morning times, the electric field in the EEJ is westward as indicated by the presence of CEJ at these times. It will be quite interesting to investigate the distinct differences between the afternoon and morning time occurrences of  $E_{sb}$  layers.

*Acknowledgements.* This work was supported by Department of Space, Government of India. One of the authors, V. Sreeja, gratefully acknowledges the financial assistance provided by the Indian Space Research Organization through Junior Research Fellowship.

Topical Editor M. Pinnock thanks E. B. Shume and another referee for their help in evaluating this paper.

## References

- Abdu, M. A., Batista, I. S., Muralikrishna, P., and Sobral, J. H. A.: Long term changes in the sporadic E-layer and electric fields over Fortaleza, Brazil, *Geophys. Res. Lett.*, 23, 757–760, 1996.
- Ananda Rao, B. G. and Raghava Rao, R.: Structural changes in the current fields of the equatorial electrojet due to zonal and meridional winds, *J. Geophys. Res.*, 92, 2514–2526, 1987.
- Anderson, D., Anghel, A., Yumoto, K., Ishitsuka, M., and Kudeki, E.: Estimating daytime vertical ExB drift velocities in the equatorial F-region using ground-based magnetometer observations, *Geophys. Res. Lett.*, 29, 1596, doi:10.1029/2001GL014562, 2002.
- Balsley, B. B.: Electric fields in the equatorial ionosphere: A review of techniques and measurements, *J. Atmos. Terr. Phys.*, 35, 1035–1044, 1973.
- Balsley, B. B. and Farley, D. T.: Radar observations of two-dimensional turbulence in the equatorial electrojet, *J. Geophys. Res.*, 78, 7471–7479, 1973.
- Buneman, O.: Excitation of field aligned sound waves by electron streams, *Phys. Rev. Lett.*, 10, 285–287, 1963.
- Crochet, M., Hanuise, C., and Broche, P.: HF radar studies of two-stream instability during an equatorial counter electrojet, *J. Geophys. Res.*, 84, 5223–5233, 1979.
- Devasia, C. V., Jyoti, N., Subbarao, K. S. V., Tiwari, D., Raghava Reddi, C., and Sridharan, R.: On the role of vertical electron density gradients in the generation of type II irregularities associated with blanketing  $E_s(E_{sb})$  during counter equatorial electrojet events: A case study, *RadioScience*, 39, RS3007, doi:10.1029/2002RS002725, 2004.
- Devasia, C. V.: Blanketing sporadic-E characteristics at the equatorial stations of Trivandrum and Kodaikanal, *Indian J. Radio Space Phys.*, 5, 217–220, 1976.
- Farley, D. T.: Theory of equatorial electrojet plasma waves: New developments and current status, *J. Atmos. Terr. Phys.*, 47, 729–744, 1985.
- Farley, D. T., Fejer, B. G., and Balsley, B. B.: Radar observations of two-dimensional turbulence in the equatorial electrojet, 3, Night-time observations of type I waves, *J. Geophys. Res.*, 83, 5625–5632, 1978.
- Farley, D. T. and Balsley, B. B.: Instabilities in the equatorial electrojet, *J. Geophys. Res.*, 78, 227–239, 1973.
- Farley, D. T.: A plasma instability resulting in field-aligned irregularities in the ionosphere, *J. Geophys. Res.*, 68, 6083–6097, 1963.
- Fejer, B. G. and Kelley, M. C.: Ionospheric irregularities, *Rev. Geophys.*, 18, 401–454, 1980.
- Fejer, B. G., Farley, D. T., Balsley, B. B., and Woodman, R. F.: Vertical structure of the VHF backscattering regions in the equatorial electrojet and the gradient drift instability, *J. Geophys. Res.*, 80, 1313–1324, 1975.
- Forbes, J. M. and Lindzen, R. S.: Atmospheric solar tides and their electrodynamic effects-I The global Sq current system, *J. Atmos. Terr. Phys.*, 38, 897–910, 1976a.
- Forbes, J. M. and Lindzen, R. S.: Atmospheric solar tides and their electrodynamic effects- II The equatorial electrojet, *J. Atmos. Terr. Phys.*, 38, 911–920, 1976b.
- Hanuise, C., Mazaudier, C., Vila, P., Blanc, M., and Crochet, M.: Global dynamo simulation of ionospheric currents and their connection with the equatorial electrojet and counter electrojet: A

- case study, *J. Geophys. Res.*, 88, 253–270, 1983.
- Krishna Murty, B. V. and Sen Gupta, K.: Disappearance of equatorial Es associated with magnetic field depressions, *Planet. Space Sci.*, 20, 371–378, 1972.
- Kudeki, E. and Sürücü, F.: Radar interferometric imaging of field-aligned plasma irregularities in the equatorial electrojet, *Geophys. Res. Lett.*, 18, 41–44, 1991.
- Kudeki, E. and Farley, D. T.: Aspect sensitivity of equatorial electrojet irregularities and theoretical implications, *J. Geophys. Res.*, 94, 426–434, 1989.
- Kudeki, E., Fejer, B. G., Farley, D. T., and Hanuise, C.: The condor equatorial electrojet campaign: Radar results, *J. Geophys. Res.*, 92, 13 561–13 577, 1987.
- Kudeki, E., Farley, D. T., and Fejer, B. G.: Theory of spectral asymmetries and nonlinear currents in the equatorial electrojet, *J. Geophys. Res.*, 90, 429–436, 1985.
- Kudeki, E., Farley, D. T., and Fejer, B. G.: Long wavelength irregularities in the equatorial electrojet, *Geophys. Res. Lett.*, 9, 684–687, 1982.
- Marriott, R. T., Richmond, A. D., and Venkateswaran, S. V.: On quiet-time equatorial electrojet and counter electrojet, *J. Geomagn. Geoelectr.*, 31, 311–340, 1979.
- Mayaud, P. N.: The equatorial counter electrojet-A review of its geomagnetic aspects, *J. Atmos. Terr. Phys.*, 39, 1055–1070, 1977.
- Rogister, A. and D'Angelo, N.: Type II irregularities in the equatorial electrojet, *J. Geophys. Res.*, 75, 3879–3887, 1970.
- Rastogi, R. G.: The equatorial electrojet: Magnetic and ionospheric effects, *Geomagnetism*, 3, 461–525, Academic Press, Sandigo, Calif, 1989.
- Rastogi, R. G., Chandra, H., and Chakravarty, S. C.: The disappearance of equatorial Es and the reversal of electrojet current, *Proc. Indian Acad. Sci.*, 74, 62–67, 1971.
- Reddy, C. A.: The equatorial electrojet, *Pure Appl. Geophys.*, 131, 485–508, 1989.
- Reddy, C. A. and Devasia, C. V.: Height and latitude structure of electric fields and currents due to local east-west winds in the equatorial electrojet, *J. Geophys. Res.*, 86, 5751–5767, 1981.
- Reddy, C. A. and Devasia, C. V.: VHF radar observation of gradient instabilities associated with blanketing Es layers in the equatorial electrojet, *J. Geophys. Res.*, 82, 125–128, 1977.
- Reddy, C. A. and Devasia, C. V.: Formation of blanketing sporadic E layers at the magnetic equator due to horizontal wind shears, *Planet. Space Sci.*, 21, 811–817, 1973.
- Richmond, A. D.: Equatorial electrojet-I. Development of a model including winds and instabilities, *J. Atmos. Terr. Phys.*, 35, 1083–1103, 1973.
- Rishbeth, H. and Garriott, O. K.: Introduction to ionospheric Physics, p. 199, Academic New York, 1969.
- Smith, L. G.: Rocket observations of sporadic E and related features of the E region, *Radio Sci.*, 1, 178–186, 1966.
- Somayajulu, V. V., Selvamurugan, R., Devasia, C. V., and Cherian, L.: VHF backscatter radar observations of type-I waves during a counter electrojet event, *Geophys. Res. Lett.*, 21, 2047–2050, 1994.
- Somayajulu, V. V. and Viswanathan, K. S.: VHF radar observations during equatorial counter electrojet events, *Indian J. Radio Space Phys.*, 16, 380–383, 1987.
- Stening, R. J., Meek, C. E., and Manson, A. H.: Upper atmosphere wind systems during reverse equatorial electrojet events, *Geophys. Res. Lett.*, 23, 3243–3246, 1996.
- Stening, R. J.: What drives the equatorial electrojet, *J. Atmos. Terr. Phys.*, 57, 1117–1128, 1995.
- Stening, R. J.: Modelling the Equatorial Electrojet, *J. Geophys. Res.*, 90, 1705–1719, 1985.
- Woodman, R. F. and Chau, J. L.: First Jicamarca radar observations of two-stream E-region irregularities under daytime counter electrojet conditions, *J. Geophys. Res.*, 107(A12), 1482, doi:10.1029/2002JA009362, 2002.